

Error mitigation for universal gates on encoded qubits

Christophe Piveteau^{1,2}, David Sutter¹, Sergey Bravyi³, Jay M. Gambetta³, and Kristan Temme³

¹*IBM Quantum, IBM Research – Zurich, Switzerland*

²*Institute for Theoretical Physics, ETH Zurich, Switzerland*

³*IBM Quantum, IBM T.J. Watson Research Center, Yorktown Heights, US*

Abstract

The Eastin-Knill theorem states that no quantum error correcting code can have a universal set of transversal gates. For self-dual CSS codes that can implement Clifford gates transversally it suffices to provide one additional non-Clifford gate, such as the T -gate, to achieve universality. Common methods to implement fault-tolerant T -gates like magic state distillation generate a significant hardware overhead that will likely prevent their practical usage in the near-term future. Recently methods have been developed to mitigate the effect of noise in shallow quantum circuits that are not protected by error correction. Error mitigation methods require no additional hardware resources but suffer from a bad asymptotic scaling and apply only to a restricted class of quantum algorithms. In this work, we combine both approaches and show how to implement encoded Clifford+ T circuits where Clifford gates are protected from noise by error correction while errors introduced by noisy encoded T -gates are mitigated using the quasi-probability method. As a result, Clifford+ T circuits with a number of T -gates inversely proportional to the physical noise rate can be implemented on small error-corrected devices without magic state distillation. We argue that such circuits can be out of reach for state-of-the-art classical simulation algorithms.

1 Introduction

The universally accepted approach to remedy effects of noise and decoherence in quantum computing is the use of quantum error correction [36, 39, 9]. The celebrated *threshold theorem* guarantees that errors in a quantum computation can be suppressed efficiently to any level for arbitrarily long circuits, if the noise rate of the physical gates is below some *constant* threshold value [2]. The low noise thresholds and the polylogarithmic qubit overhead needed to implement error correction protocols are very demanding on the quantum hardware. However, the by far largest overhead for quantum algorithms with current error correcting codes stems from the implementation of a fault-tolerant universal gate set.

For gates that can be implemented *transversally* the overhead is manageable, because by definition these gates are fault-tolerant as they do not spread errors within code blocks. The Eastin-Knill theorem proves that no quantum error correcting code can transversally implement a universal set of gates [13]. It is known that self-dual CSS codes can implement the entire Clifford group transversally [37]. To obtain a universal gate set a single further non-Clifford gate is needed. One commonly used gate that completes the group to a universal gate set is the T -gate.

A common approach to implement the T -gate fault-tolerantly is the use of reliable encoded magic-states [6]. These states can be prepared by a technique called *magic state distillation* and every encoded magic state can be used to perform a T -gate using only Clifford operations as shown in Figure 1. The distillation of magic states is responsible for the largest overhead in a fault-tolerant computing system.

While the hardware requirements to implement quantum algorithms fault-tolerantly have not been met yet, steady progress in the development of quantum hardware has been made [18, 11, 8]. This has given rise to the question: Are there computational tasks that could be implemented without the use of quantum error correction? This question has motivated a set of proposals [32, 21, 16, 35, 26, 27]

that only ask for the implementation of shallow quantum circuits and the estimation of expectation values. Early experimental implementations [29, 19, 20, 16, 33] of such proposals have shown that the effect of decoherence on the result is non-negligible, despite the use of the restrictive computational models and good noise levels. It has become clear that methods to remove the noise induced biased from the expectation values need to be applied. These methods are referred to as *quantum error mitigation* [40, 24] and have the advantage of not requiring additional qubit resources and can be implemented directly on noisy hardware. However, these techniques are only able to systematically remove the bias from the expectation values and cannot extend the coherence times of the computation. This manifests in a bad asymptotic scaling of most error mitigation methods emphasizing that such techniques are most favorable for near-term circuits.

Given the significant hardware overhead required for the implementation of a fault-tolerant universal gate set it is meaningful to investigate the possibility of using error mitigation techniques to reduce this overhead in circuits using encoded qubits for the estimation of expectation values. In this work, we present two methods to mitigate the bias induced by noisy encoded T -gates using the *quasi-probability decomposition* (QPD) method [40]. Both approaches circumvent the need for magic state distillation. The cost of the QPD method is an increased number of required shots to guarantee a fixed accuracy. For a single gate, this increase scales as γ_ε^2 where $\gamma_\varepsilon \geq 1$ is a quantity called *sampling overhead* that captures the non-negativity of the quasi-probability decomposition. The sampling overhead depends on the error rate ε of the physical gates and on the error correcting code used for the encoding. It grows multiplicatively in the number of T -gates or T -count. For a circuit with T -count t , the total sampling overhead is $\Gamma_\varepsilon := \gamma_\varepsilon^t$. In the limit $\varepsilon \rightarrow 0$ the sampling overhead disappears, i.e., $\lim_{\varepsilon \rightarrow 0} \gamma_\varepsilon = 1$.

Our first method is based on noisy magic state preparation which has a favourable scaling of the sampling overhead but requires two logical qubits to simulate a logical T -gate. The second approach is based on code switching and requires a single logical qubit only, however at the cost of a larger sampling overhead. The two proposals achieve a sampling cost that scales as $\gamma_\varepsilon = 1 + 2\kappa\varepsilon + O(\varepsilon^2)$, where κ denotes a universal constant that varies for the two methods and depends on the considered error model as well as on the error correcting code. For realistic scenarios we find that $\kappa \approx 2/5$ and $\kappa \leq 30$ for the first and second method, respectively.

As a result, assuming that we fix some value of the total sampling cost Γ_ε^2 that the user is willing to accept, we can simulate the outcome of a universal fault-tolerant quantum circuits with a T -count up to $\eta/\varepsilon + O(1)$, where $\eta := \log(\Gamma_\varepsilon^2)/(4\kappa)$. More concretely, for a physical error rate $\varepsilon = 10^{-2}$ and total sampling cost $\Gamma_\varepsilon^2 = 10^3$ we can simulate outcomes for circuits with up to 200 T -gates. In case of further experimental progress such that $\varepsilon = 10^{-3}$ we can go up to 2000 T -gates. We refer to Figure 6 for more details and the precise calculations. This considerably exceeds the possibilities of state of the art classical algorithms to simulate universal quantum circuits [4, 31] which can deal with approximately 50 T -gates.

2 Error-mitigated logical T-gates via noisy magic states

In this section we present an approach of how to error-mitigate a logical T -gate, i.e., $T = \text{diag}(1, e^{i\pi/4})$, which is implemented using noisy magic states. This approach uses two logical qubits and combines ideas from error correction with quantum error mitigation.

2.1 Noisy magic state preparation

One possibility to implement a T -gate is via a Clifford circuit shown in Figure 1 and the presence of a magic state

$$|\pi/4\rangle = \frac{1}{\sqrt{2}}(|0\rangle + e^{i\pi/4}|1\rangle).$$

This approach reduces the problem of implementing a fault-tolerant T -gate to the task of a fault-tolerant preparation of encoded magic states. The latter task can be achieved by magic state distillation [6], where several noisy magic states are transformed into fewer magic states of better fidelity. Whereas magic state distillation is a very elegant approach for achieving universal fault-tolerant quantum computing, the distillation process leads to a considerable overhead in practice. In our method we forego the usage of magic state distillation and make use of the same circuit in Figure 1 with a noisy magic state. This will lead to a faulty T -gate. In a second step, we use quantum error mitigation techniques, such as the QPD method, to suppress this error.

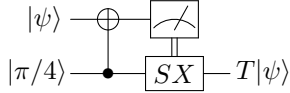


Figure 1: **Implementation of a T -gate** via a magic state $|\pi/4\rangle$ and Clifford operations. The S and X gates are only performed if the measurement outcome is 1.

Let ρ be a noisy encoded magic state. We define the logical error rate as

$$\bar{\varepsilon} := 1 - \langle \pi/4 | \rho | \pi/4 \rangle. \quad (1)$$

For simplicity, assume that the chosen error correction code enables a noiseless implementation of logical gates $S = \text{diag}(1, i)$, X , CNOT, preparation of logical $|0\rangle$ and $|+\rangle$ states, and measurements of a logical qubit in the Z and X basis.¹ We can twirl the noisy magic state ρ with respect to the group $\{I, A\}$, where A is the Clifford gate defined as

$$A := e^{-i\pi/4} SX = |\pi/4\rangle\langle\pi/4| - |\omega\rangle\langle\omega|,$$

where $|\omega\rangle := Z|\pi/4\rangle$ is a state orthogonal to $|\pi/4\rangle$ and I denotes the identity. The twirled state thus becomes

$$\tau := \frac{1}{2}(\rho + A\rho A^\dagger) = (1 - \bar{\varepsilon})|\pi/4\rangle\langle\pi/4| + \bar{\varepsilon}|\omega\rangle\langle\omega|, \quad (2)$$

where the second equality follows from the identity $A|\pi/4\rangle\langle\omega|A^\dagger + |\pi/4\rangle\langle\omega| = 0$. Thus we can prepare the twirled state τ by first preparing ρ and then applying the logical A gate with probability 1/2. The twirled state τ can be considered as the ideal magic state $|\pi/4\rangle$ that suffers from a random Pauli Z error applied with probability $\bar{\varepsilon}$, since $|\omega\rangle = Z|\pi/4\rangle$.

Note that a Pauli Z error on the magic state $|\pi/4\rangle$ has no effect on the measurement in Figure 1. Thus using the twirled state τ instead of the ideal magic state $|\pi/4\rangle$ inside the T -gate gadget in Figure 1, one can implement a noisy T -gate

$$\mathcal{T}_{\bar{\varepsilon}} = (1 - \bar{\varepsilon})\mathcal{T} + \bar{\varepsilon}\mathcal{Z} \circ \mathcal{T}, \quad (3)$$

where \mathcal{T} and \mathcal{Z} denote the quantum channels implementing the ideal T - and Z -gate, respectively, i.e., $\mathcal{T}(B) = TBT^\dagger$ and $\mathcal{Z}(B) = ZBZ^\dagger$ for any single qubit operator B . We next want to use error mitigation techniques to simulate a perfect T -gate described by the channel \mathcal{T} using the noisy T -gate described by the channel $\mathcal{T}_{\bar{\varepsilon}}$. To do so we need to have a good estimate for the logical error rate $\bar{\varepsilon}$. This could be done via standard tomography techniques, however we present a more efficient method in the next section.

It remains to understand how the logical error rate $\bar{\varepsilon}$ defined in (1) depends on the physical error rate ε . It has been shown [25] that there exist noisy state preparation circuits for the surface code that prepare a noisy encoded magic state ρ such that the logical error rate is upper bounded by a constant

¹This assumption can be forced to hold by choosing a code that has a sufficiently large distance. Note that these gates are Clifford gates that feature a transversal and hence fault-tolerant implementation for self-dual CSS codes.

that is independent of the code distance [25]. In fact $\bar{\varepsilon}$ can be in the same order as the physical error rate ε . For the surface code and a depolarizing error model it has been shown [23] that

$$\bar{\varepsilon} = \kappa \varepsilon + O(\varepsilon^2), \quad (4)$$

where κ is a conversion constant that depends on the details of the noise model. For example, in case of perfect single qubit gates and no initialization errors we find $\kappa = 2/5$ [23]. Furthermore, the second order term in (4) is negligible for realistic error rates.²

The standard Kitaev's surface code does not feature a transversal logical S -gate because it is not a self-dual CSS code. In fact, it is known that the surface code does not permit logical non-Pauli gates realizable by geometrically local constant-depth circuits [3, Theorem 7.1]. As a result, it is not clear how to implement the logical Clifford operator A required for the twirling (2). Luckily any logical single-qubit Clifford gate for the surface code can be implemented by a constant depth circuit with long-range gates [28, 5]. Any constant-depth circuit is automatically fault-tolerant even if it is not geometrically local. Indeed, the constant depth condition implies that a single fault in the circuit can affect only a constant number of output qubits. This gives a fault-tolerant implementation of the S -gate for the Kitaev's surface code.

2.2 Learning the logical error rate

The goal of this section is to describe an efficient method to experimentally measure the logical error rate $\bar{\varepsilon}$. To do so we define a phase flip channel

$$\mathcal{N}_{\bar{\varepsilon}} := (1 - \bar{\varepsilon})\mathcal{I} + \bar{\varepsilon}\mathcal{Z}, \quad (5)$$

where \mathcal{I} denotes the identity channel. Since \mathcal{T} and \mathcal{Z} commute we have for any $p \in \mathbb{N}$

$$\mathcal{T}_{\bar{\varepsilon}}^p = (\mathcal{N}_{\bar{\varepsilon}} \circ \mathcal{T})^p = \mathcal{N}_{\bar{\varepsilon}}^p \circ \mathcal{T}^p. \quad (6)$$

For $p \equiv 0 \pmod{8}$ we have $T^p = \mathbf{1}$ and $\mathcal{T}^p = \mathcal{I}$. Hence (6) ensures that $\mathcal{T}_{\bar{\varepsilon}}^p = \mathcal{N}_{\bar{\varepsilon}}^p$. We can now learn the logical error rate $\bar{\varepsilon}$ by preparing a logical state $|+\rangle$ fault-tolerantly, applying $\mathcal{T}_{\bar{\varepsilon}}^p$ and measuring the output in the $\{|+\rangle, |-\rangle\}$ basis, which gives us an outcome 1 or 0. We repeat this circuit many times to estimate the expectation value of the outcome, which we denote by

$$f(p) := \langle + | \mathcal{T}_{\bar{\varepsilon}}^p (|+\rangle\langle+|) | + \rangle = \langle + | \mathcal{N}_{\bar{\varepsilon}}^p (|+\rangle\langle+|) | + \rangle = \frac{1}{2} \left(1 + (1 - 2\bar{\varepsilon})^p \right),$$

where the final step can be checked with a simple iterative argument. By measuring $f(p)$ for $p = 8k$ with $k \in \mathbb{N}$, we can obtain a good estimate for $\bar{\varepsilon}$ using exponential fitting. Once we learned the logical error rate $\bar{\varepsilon}$ we can use various error mitigation techniques, such as the QPD method, to transform the noisy T -gate $\mathcal{T}_{\bar{\varepsilon}}$ into a good approximation of the perfect T -gate \mathcal{T} , which is discussed next.

2.3 Reducing noise using the quasi-probability decomposition method

The QPD method is a quantum error mitigation technique introduced in [40]. It allows for the simulation of an arbitrary channel \mathcal{F} (e.g. an ideal quantum gate) while only having access to quantum hardware that can execute the noisy quantum channels $\{\mathcal{E}_i\}$. The central ingredient of the method is a decomposition

$$\mathcal{F} = \sum_i a_i \mathcal{E}_i, \quad (7)$$

²The protocol in [23] uses post-selection to suppress logical error with a relatively large success rate. Hence the cost of this step is modest. More information can be found in [23].

where the $a_i \in \mathbb{R}$ are quasi-probability coefficients. During execution of the circuit, the gate is probabilistically replaced with one of the channels \mathcal{E}_i with probability $|a_i|/\gamma$ where $\gamma := \sum_i |a_i|$. By correctly weighting the measurement outcome at the end of the circuit, one can obtain an unbiased estimate of the true expectation value of the outcome of the ideal quantum circuit by performing Monte Carlo sampling. The number of samples required to reach a certain accuracy $\delta > 0$ scales as $\mathcal{O}(\gamma^2/\delta^2)$. We therefore call γ the *sampling overhead* of the QPD method. More information about the QPD method can be found in [40, 14, 34].

We can express the perfect T -gate \mathcal{T} in terms of the noisy T -gate $\mathcal{T}_{\bar{\varepsilon}}$ by using the identity

$$\mathcal{T} = \left(\frac{1 - \bar{\varepsilon}}{1 - 2\bar{\varepsilon}} \right) \mathcal{T}_{\bar{\varepsilon}} - \left(\frac{\bar{\varepsilon}}{1 - 2\bar{\varepsilon}} \right) \mathcal{Z} \circ \mathcal{T}_{\bar{\varepsilon}}, \quad (8)$$

which gives us a QPD of the form (7) with $\mathcal{E}_1 = \mathcal{T}_{\bar{\varepsilon}}$, $\mathcal{E}_2 = \mathcal{Z} \circ \mathcal{T}_{\bar{\varepsilon}}$, $a_1 = (1 - \bar{\varepsilon})/(1 - 2\bar{\varepsilon})$, and $a_2 = -\bar{\varepsilon}/(1 - 2\bar{\varepsilon})$. We thus see that the sampling overhead is given by

$$\gamma = |a_1| + |a_2| = \frac{1}{1 - 2\bar{\varepsilon}}.$$

Expanding this term around $\bar{\varepsilon} = 0$ gives

$$\gamma_{\varepsilon} = 1 + 2\bar{\varepsilon} + O(\bar{\varepsilon}^2) = 1 + 2\kappa\varepsilon + O(\varepsilon^2) \quad \text{if } \bar{\varepsilon} \ll 1 \quad \text{and } \varepsilon \ll 1, \quad (9)$$

where κ denotes a conversion constant that depends on the used error-correcting code as well as on the error model. The final step in (9) uses the fact that it is possible to do encoding such that the logical error rate $\bar{\varepsilon}$ is proportional to the physical error rate ε up to quadratic terms, in the sense of (4). To keep our framework general we treat κ an arbitrary constant so that various codes or underlying physical error models fit our setting.

3 Error-mitigated logical T-gates via code switching

The implementation of a T -gate via magic states (see Figure 1) has the drawback of using two encoded qubits. It also includes a logical CNOT gate which may require more logical qubits for certain implementations [17]. One may ask if a logical T -gate can be implemented using only one logical qubit. In this section we show how to accomplish this task by combining the QPD method and the code switching method pioneered by Paetznick and Reichardt [30].

3.1 The idea of code switching

Suppose \mathcal{S}_1 and \mathcal{S}_2 are CSS-type [9, 38] quantum codes with one logical qubit. Our goal is to implement a logical T -gate on a qubit encoded by \mathcal{S}_1 . We assume that \mathcal{S}_1 has a large distance for both X and Z errors and enables a fault-tolerant implementation of the Clifford gate $S = T^2$. We assume that \mathcal{S}_2 is an asymmetric code with a large distance for X errors and a small distance for Z errors such that a logical- Z operator of \mathcal{S}_2 can be chosen as a single-qubit Pauli Z on some physical qubit. We shall denote this local logical- Z operator as \bar{Z}_{loc} . This allows us to perform a logical T -gate on a qubit encoded by \mathcal{S}_2 simply by applying a physical T -gate on the qubit acted upon by \bar{Z}_{loc} . Indeed, since the T -gate is a linear combination of the identity and the Pauli Z , the physical and the logical T -gates become equivalent. The code switching method enables a conversion between the codes \mathcal{S}_1 and \mathcal{S}_2 by measuring stabilizers of \mathcal{S}_2 on a logical state encoded by \mathcal{S}_1 or vice versa. In certain cases this conversion can be performed fault-tolerantly [30]. This is achieved by identifying stabilizers present in both codes and using the measured syndromes of such stabilizers to diagnose and correct errors. The error suppression typically scales exponentially with the code distance. In our case the code switching protects the encoded qubit exponentially well only from logical X errors. This ensures that the effective noise channel acting on the logical qubit is dominated by Z -type (possibly coherent) errors. Thus the

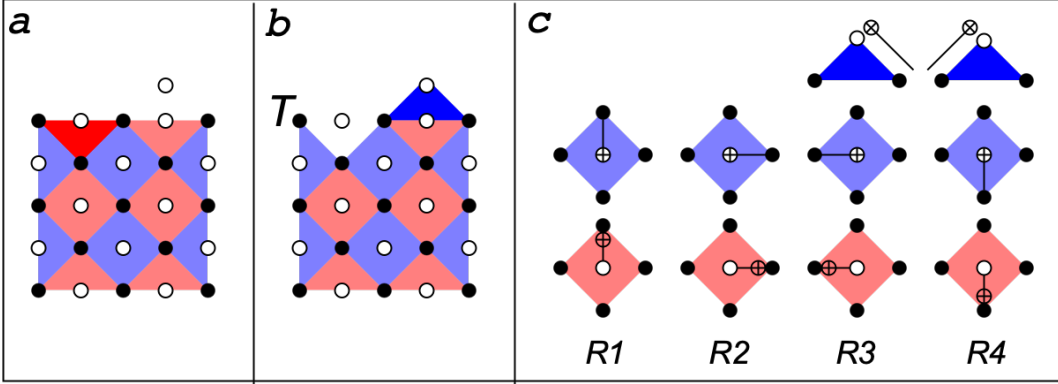


Figure 2: **Logical T -gate by code switching.** (a) Surface code \mathcal{S}_1 with the distance $d = 3$. Black and white circles indicate data and syndrome qubits. Red and blue faces indicate X and Z stabilizers. (b) Asymmetric surface code \mathcal{S}_2 exhibiting a single-qubit logical T -gate at the north-west corner of the lattice. Code switching $\mathcal{S}_1 \rightarrow \mathcal{S}_2$ is performed by turning off X stabilizer F_1 (dark red triangle) and turning on Z stabilizer G_1 (dark blue triangle). (c) The syndrome extraction cycle consists of four rounds of CNOTs $R1, R2, R3, R4$. To avoid clutter we only show a local schedule of CNOTs for each stabilizer. Schedules for weight-3 stabilizers are properly truncated. The schedule extends to the full lattice in a translation invariant fashion.

code switching implements a noisy logical T -gate of the form $\mathcal{T}_n = \mathcal{N} \circ \mathcal{T}$ where \mathcal{N} is some Z -type noise channel. We can tailor this noise to become stochastic Z noise by twirling over the X gate using the identity

$$\frac{1}{2}(\mathcal{N} + \mathcal{X} \circ \mathcal{N} \circ \mathcal{X}) = (1 - \bar{\varepsilon})\mathcal{I} + \bar{\varepsilon}\mathcal{Z} =: \mathcal{N}_{\bar{\varepsilon}},$$

for some logical error rate $\bar{\varepsilon}$ where $\mathcal{X}(B) = XBX^\dagger$ for any single qubit operator B . Using the identity $XT = TA$ we get

$$\frac{1}{2}(\mathcal{T}_n + \mathcal{X} \circ \mathcal{T}_n \circ \mathcal{A}) = \mathcal{N}_{\bar{\varepsilon}} \circ \mathcal{T} = \mathcal{T}_{\bar{\varepsilon}}, \quad (10)$$

where $\mathcal{A}(B) = ABA^\dagger$ for any single qubit operator B and $\mathcal{T}_{\bar{\varepsilon}}$ is defined as in (3). By assumption, the code \mathcal{S}_1 enables a fault-tolerant implementation of the Pauli X and the S gate on the encoded qubit. Since $A = SX$ up to an overall phase, the twirling in (10) can be implemented fault-tolerantly on a qubit encoded by \mathcal{S}_1 by applying either \mathcal{T}_n or $\mathcal{X} \circ \mathcal{T}_n \circ \mathcal{A}$ with the probability 1/2 each. Since at this point we have implemented a noisy T -gate of the form $\mathcal{T}_{\bar{\varepsilon}}$, we can follow the procedure from Section 2.2 to determine the parameter $\bar{\varepsilon}$ efficiently. The error mitigation procedure is completely analogous to the description in Section 2.3.

3.2 Detailed construction for Kitaev's surface code

We shall now specialize the code switching method to Kitaev's surface code [22] depicted on Figure 2. A distance- d code surface code is defined on a square lattice of linear size $2d - 1$. Code qubits live at sites indicated by black circles on Figure 2. Let \mathcal{S}_1 be the stabilizer group of the surface code generated by X and Z stabilizers located on red (X) and blue (Z) faces of the lattice, see Figure 2. We choose logical Pauli operators \overline{X} and \overline{Z} as products of single-qubit X and Z along the left (X) and the top (Z) boundary.

Next let us define an asymmetric version of the surface code with a small distance for Z errors. Its stabilizer group \mathcal{S}_2 is obtained from \mathcal{S}_1 by introducing some new Z stabilizers and removing some

X stabilizers. This modification only affects stabilizers located near the top boundary, as shown on Figure 2. To describe this formally, let $d = 2t+1$ be the code distance. Label code qubits located at the top boundary by integers $1, 2, \dots, d$ in the order from the left to the right such that $\bar{Z} = Z_1 Z_2 \cdots Z_d$. Define Pauli operators

$$G_i := Z_{2i} Z_{2i+1}.$$

The group \mathcal{S}_2 is obtained from \mathcal{S}_1 by adding t new stabilizers G_1, \dots, G_t and removing every second X stabilizer adjacent to the top boundary, see Figure 2 for an example. An X stabilizer of \mathcal{S}_1 is removed if it anti-commutes with some operator G_i . Let $q_{\text{loc}} := 1$ be the data qubit located at the north-west corner of the lattice. The code \mathcal{S}_2 exhibits a local logical- Z operator acting only on the qubit q_{loc} , namely

$$\bar{Z}_{\text{loc}} = \bar{Z} \prod_{i=1}^t G_i = Z_{q_{\text{loc}}}. \quad (11)$$

Note that \bar{Z}_{loc} and \bar{Z} differ by stabilizers of \mathcal{S}_2 and thus have the same action on any logical state of \mathcal{S}_2 . Thus the logical T -gate on a qubit encoded by \mathcal{S}_2 can be implemented by either of the following operators:

$$\bar{T} = e^{-i\frac{\pi}{8}\bar{Z}} \quad \text{and} \quad \bar{T}_{\text{loc}} = e^{-i\frac{\pi}{8}\bar{Z}_{\text{loc}}}. \quad (12)$$

Here we ignore the overall phase. Note that \bar{T} also implements a logical T -gate for the code \mathcal{S}_1 since both codes have the same logical Pauli operators. Let $\mathcal{G} = \langle G_1, \dots, G_t \rangle$ be the group generated by G_1, \dots, G_t . We claim that a logical T -gate on a qubit encoded by the surface code \mathcal{S}_1 can be implemented as follows.

Algorithm 1 Logical T -gate by code switching

- 1: Initialize code qubits in a logical state of the surface code \mathcal{S}_1
- 2: Measure the syndrome of the asymmetric surface code \mathcal{S}_2
- 3: Let σ_i be the measured syndrome of G_i
- 4: Compute $\sigma = \prod_{i=1}^t \sigma_i$
- 5: Apply a single-qubit operator $(\bar{T}_{\text{loc}})^\sigma$ to the post-measurement state
- 6: Measure the syndrome of the surface code \mathcal{S}_1
- 7: Compute a Pauli operator $R \in \mathcal{G}$ consistent with the measured syndrome of \mathcal{S}_1
- 8: Apply R to the post-measurement state

Indeed, let $|\psi_j\rangle$ be a state obtained after executing the first j steps of this algorithm. We need to show that $|\psi_8\rangle = \bar{T}|\psi_1\rangle$. Let Π be a projector describing the measurement at step 2 such that $|\psi_2\rangle = \Pi|\psi_1\rangle$, ignoring the normalization. From $G_i|\psi_2\rangle = \sigma_i|\psi_2\rangle$ and (11),(12) one infers $(\bar{T}_{\text{loc}})^\sigma|\psi_2\rangle = \bar{T}|\psi_2\rangle$. Since \bar{Z} is a logical operator for both codes \mathcal{S}_i , the logical gate \bar{T} commutes with the syndrome measurement of \mathcal{S}_2 . Thus

$$|\psi_5\rangle = (\bar{T}_{\text{loc}})^\sigma|\psi_2\rangle = \bar{T}|\psi_2\rangle = \Pi\bar{T}|\psi_1\rangle.$$

Let Λ be a projector describing the measurement at step 6. In the absence of errors the measured syndrome is non-trivial only for stabilizers of \mathcal{S}_1 that anti-commute with some element of \mathcal{S}_2 . One can check that there are exactly t such stabilizers which we denote F_1, \dots, F_t . The stabilizer F_i acts on data qubits $2i-1, 2i$ located at the top boundary as well as the data qubit located at the second row between $2i-1$ and $2i$, see Figure 2. Let $\lambda_i \in \{1, -1\}$ be the syndrome of F_i measured at step 6. The operator R used at step 7 is defined as

$$R = \prod_{i: \lambda_i = -1} \prod_{a=i}^t G_a.$$

Using the commutation rules between the operators F_i and G_a one can easily check that R has the syndrome λ , that is, $RF_i = \lambda_i F_i R$ for all $i = 1, \dots, t$. Write $\Lambda = R\Gamma R$, where Γ is a projector onto the logical subspace of the surface code \mathcal{S}_1 . The above shows that

$$|\psi_8\rangle = R\Lambda|\psi_5\rangle = (R\Lambda R)R|\psi_5\rangle = \Gamma R|\psi_5\rangle = \Gamma R\Pi\bar{T}|\psi_1\rangle = \Gamma(R\Pi)\Gamma\bar{T}|\psi_1\rangle.$$

To obtain the last equality we noted that $\Gamma|\psi_1\rangle = |\psi_1\rangle$ and that \bar{T} commutes with Γ . The operator $R\Pi$ is a linear combination of Pauli operators from the group $\mathcal{S}_1 \cdot \mathcal{G}$. One can easily check that this group contains only stabilizers of the surface code and detectable errors. Thus $\Gamma(R\Pi)\Gamma$ is proportional to Γ . The latter has trivial action on the logical state $\bar{T}|\psi_1\rangle$. This proves that $|\psi_8\rangle = \bar{T}|\psi_1\rangle$, as claimed.

We make Algorithm 1 partially fault-tolerant by repeating syndrome measurements at step 2 and step 6 sufficiently many times. The observed syndromes are used to compute an error-corrected version of the phase σ at step 4 and to perform the final error correction after step 8. Accordingly, the algorithm can fail in two distinct ways. First, the final state could be $(\bar{T})^{-1}|\psi_1\rangle$ instead of $\bar{T}|\psi_1\rangle$ because some syndrome σ_i has been flipped due to an error. Such error results in a wrong phase σ computed at step 4. We shall refer to such events as Pauli frame errors since they can be viewed as applying the T -gate in a wrong Pauli frame. Likewise, an undetected X error that occurs before step 5 on the qubit q_{loc} would result in a Pauli frame error, as can be seen from the identity $\bar{T}_{\text{loc}}X_1 = X_1(\bar{T}_{\text{loc}})^{-1}$. Secondly, the algorithm may fail if the final error correction performed after step 8 resulted in a logical error. We would like to achieve an exponential suppression for logical X errors and, at the same time, ensure that Pauli frame and logical Z errors occur with probability at most $\kappa\varepsilon$, where ε is the physical error rate and κ is a constant prefactor.

To measure the syndrome of the surface code \mathcal{S}_1 we use a well-known quantum circuit proposed in [12, 15]. It requires one ancillary syndrome qubit per each stabilizer, see Figure 2. The circuit applies four rounds of CNOTs that compute the syndrome of each stabilizer into the respective syndrome qubit. A syndrome measurement cycle begins by resetting each syndrome qubit to $|0\rangle$ or $|+\rangle$ state for Z and X stabilizers respectively. The cycle ends by measuring each syndrome qubit in the Z - or X -basis. A circuit measuring the syndrome of \mathcal{S}_2 requires only a few minor modifications, see Figure 2.

For numerical simulations we chose the depolarizing noise model [15]. It depends on a single error rate parameter ε such that each operation in the circuit (a gate, a measurement, or a qubit reset) becomes faulty with the probability ε . Faults on different operations are independent. The model can be described by stochastic Pauli errors enabling efficient simulation using the stabilizer formalism [1]. A faulty CNOT gate is modelled as the ideal CNOT followed by a Pauli error drawn uniformly at random from the two-qubit Pauli group. A faulty measurement is modelled as the ideal measurement whose outcome is flipped. A faulty qubit reset prepares a basis state orthogonal to the ideal one. A faulty idle qubit suffers from a Pauli error X , Y , or Z .

Let us first discuss how to correct Pauli frame errors. Suppose U is a quantum circuit describing the first two steps of Algorithm 1 with L syndrome measurement cycles at step 2. The circuit outputs a quantum state $|\psi_2\rangle$ and a classical syndrome history h specifying the syndrome of each stabilizer of \mathcal{S}_2 measured in each of L syndrome cycles. In the absence of errors all stabilizers except for G_1, \dots, G_t have trivial syndromes. Furthermore, the syndromes of G_i measured in different cycles are the same. Let $\mathcal{F}(U)$ be the set of all possible faulty implementations of U , as prescribed by the depolarizing noise model. Each circuit $\tilde{U} \in \mathcal{F}(U)$ differs from U by inserting Pauli errors at some space-time locations (measurement and reset errors can be modeled by inserting suitable Pauli errors before the ideal measurement and after the ideal reset). We pick a faulty circuit $\tilde{U} \in \mathcal{F}(U)$ randomly, according to the depolarizing noise model. A simulation of the circuit \tilde{U} yields a noisy syndrome history \tilde{h} . To perform error correction we used the maximum-weight matching (MWM) decoder proposed in [7] which is closely related to the one used in Refs. [12, 15]. The MWM decoder takes the syndrome history \tilde{h} as an input and outputs a candidate faulty circuit $\tilde{U}_{\text{dec}} \in \mathcal{F}(U)$ consistent with \tilde{h} . By propagating all Pauli errors contained in \tilde{U}_{dec} towards the final time step we compute error-corrected syndromes σ_i and a Pauli correction C acting on the data qubits such that $CU|\psi_1\rangle$ is our guess of the noisy state $\tilde{U}|\psi_1\rangle$, based on the available syndrome information. Step 4 of Algorithm 1 computes an

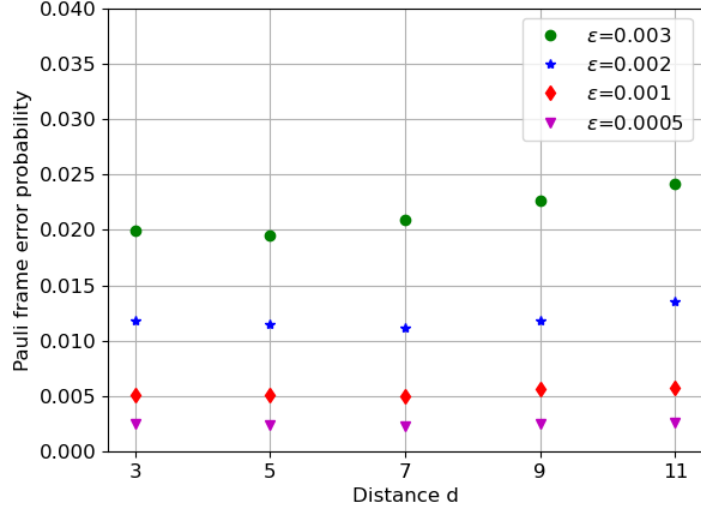


Figure 3: **Probability of a Pauli frame error** P_F for the code switching $\mathcal{S}_1 \rightarrow \mathcal{S}_2$ with $L = 3$ syndrome measurement cycles for the asymmetric surface code \mathcal{S}_2 . The initial state is chosen as an ideal logical state of the surface code \mathcal{S}_1 . A Pauli frame error in the code switching results in the implementation of the logical gate $(\bar{T})^{-1}$ instead of \bar{T} . Our data suggest a scaling $P_F \approx 6\epsilon + O(d\epsilon^2)$.

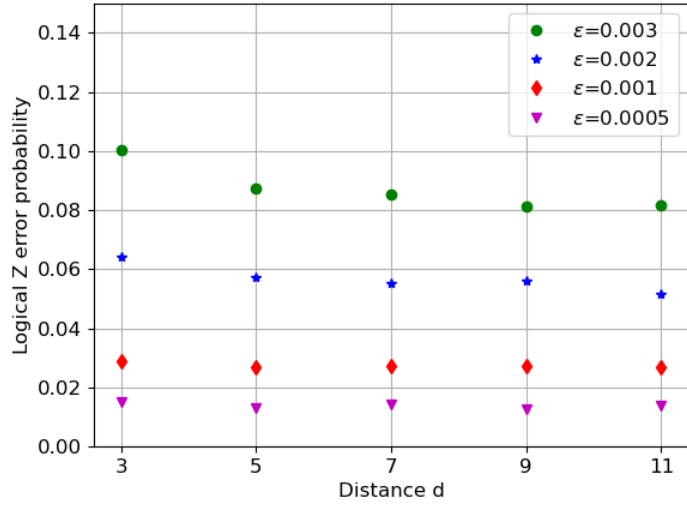


Figure 4: **Probability of a logical Z error** P_Z for the code switching $\mathcal{S}_1 \rightarrow \mathcal{S}_2 \rightarrow \mathcal{S}_1$ with $L = 3$ syndrome cycles for the asymmetric surface code \mathcal{S}_2 and d syndrome cycles for the regular surface code \mathcal{S}_1 . To enable efficient simulation we skipped the T -gate application in Algorithm 1. Our data suggests a scaling $P_Z \approx 26\epsilon$ for a large code distance. The large constant prefactor stems from leaving the logical qubit unprotected from Z errors for $L + 1$ syndrome cycles when the full syndrome information for X stabilizers of the code \mathcal{S}_1 is unavailable.

error-corrected phase $\sigma = (-1)^a \sigma_1 \cdots \sigma_t$, where $a = 1$ if C contains an X error on the qubit q_{loc} and $a = 0$ otherwise. To avoid the actual application of the T -gate (which would require non-stabilizer simulators) we chose the initial logical state $|\psi_1\rangle$ as an eigenvector of \bar{Z} , that is, $|\psi_1\rangle = |\bar{b}\rangle$, where $b \in \{0, 1\}$ is a random bit. Error correction succeeds if $\bar{U}|\psi_1\rangle$ is an eigenvector of $(\bar{T}_{\text{loc}})^{\sigma}$ with the eigenvalue $(-1)^b$. Otherwise, a Pauli frame error is declared.

Our numerical results for the probability of a Pauli frame error P_F are shown on Figure 3. Each data point represents an empirical estimate of P_F obtained by the Monte Carlo method (we used between 50,000 and 200,000 Monte Carlo trials per data point). We chose $L = 3$ syndrome measurement cycles to ensure that any single fault in the measurement of σ_i is correctable. Recall that the MWM decoder detects errors by examining differences between syndromes measured in subsequent cycles. Thus $L = 3$ provides two parity checks to diagnose errors in the three measured values of σ_i , in a way analogous to the 3-bit repetition code. In contrast, choosing $L = 2$ would only allow to detect a faulty bit σ_i but not to correct it (if the two measured values of σ_i disagree, there is no way to select the correct value). Choosing $L > 3$ is undesirable as this leaves the logical qubit unprotected from Z errors for a longer time. Our data suggests a scaling $P_F \approx 6\epsilon + O(d\epsilon^2)$. We numerically observed that the dominant contribution to P_F stems from X errors occurring on the qubit q_{loc} in the last syndrome cycle as well as syndrome measurement errors on the Z stabilizer acting on the qubit q_{loc} in the last syndrome cycle. The term $O(d\epsilon^2)$ can be understood as a result of a weight-two error affecting the measurement of some syndrome bit σ_i . Here $i = 1, \dots, t$ can be arbitrary. Such weight-two error cannot be corrected using only $L = 3$ syndrome cycles.

Finally, we estimated the probability of logical X and Z errors by simulating a simplified version of Algorithm 1 without steps 3,4,5. In other words, we skipped the application of the physical T -gate. This enables efficient simulation using the stabilizer formalism. The MWM decoder takes as input the combined syndrome history measured at steps 2,6 and calculates a Pauli correction to be applied after step 8. The standard implementation for MWM decoder [7] was properly modified to take into account that some stabilizers are turned off and on during the code switching. Namely, syndromes of the operators G_i measured in the first cycle of step 2 as well as syndromes of the operators F_i measured in the first cycle of step 6 are not used to diagnose errors. As commonly done in the literature, we chose the number of syndrome cycles for the surface code \mathcal{S}_1 equal to the code distance d and added a noiseless syndrome cycle at the end of the protocol.

Our numerical results for the probability of logical Z and X errors P_Z and P_X are shown on Figures 4 and 5, respectively. Our data suggests a scaling $P_Z \approx 26\epsilon$ for a large code distance. The large constant prefactor can be seen as the price we pay for leaving the logical qubit unprotected from Z errors during L syndrome cycles at step 2. In fact, since the syndromes of X stabilizers F_i measured in the first cycle of step 6 are random, these syndrome provide no information about Z errors that occurred in this cycle. Thus, the logical qubit is unprotected from Z errors for $L + 1 = 4$ cycles. Since each cycle is a depth-6 circuit (four CNOT rounds, reset round, and measurement round), the error correction for Z errors is effectively turned off for 24 time steps. This is in a good agreement with the scaling $P_Z \approx 26\epsilon$. Finally, we observed that the probability of logical X errors is exponentially suppressed as one increases the code distance, see Figure 5. Thus the noise in the implemented logical T -gate is dominated by (coherent) Z errors, as expected.

We anticipate the scaling of P_Z can be improved by optimizing the code switching protocol. For example, one can reduce P_Z roughly by the factor 2/3 by choosing the number of syndrome measurement cycles L for the code \mathcal{S}_2 adaptively such that $L = 2$ if the syndromes σ_i measured in the first and the second cycles are the same for all $i = 1, \dots, t$ and $L = 3$ otherwise. This would ensure that a single fault in the measurement of σ_i can be corrected, similar to the $L = 3$ implementation described above. However, the logical qubit remains unprotected from logical Z errors for a shorter time (two cycles instead of three cycles, in the limit $\epsilon \rightarrow 0$).

Under the assumption that we use a code with a sufficiently large distance, the logical X errors are negligible. Hence the logical error rate $\bar{\epsilon}$ is determined by the logical Z and Pauli frame errors. The latter are described by the channel $(1 - P_F)\mathcal{I} + P_F\mathcal{S}^{\dagger}$, where $\mathcal{S}^{\dagger}(B) = S^{\dagger}BS$ for any single qubit operator B . Twirling over the X gate gives a Z -type noise channel $(1 - P_F/2)\mathcal{I} + (P_F/2)\mathcal{Z}$. Assuming

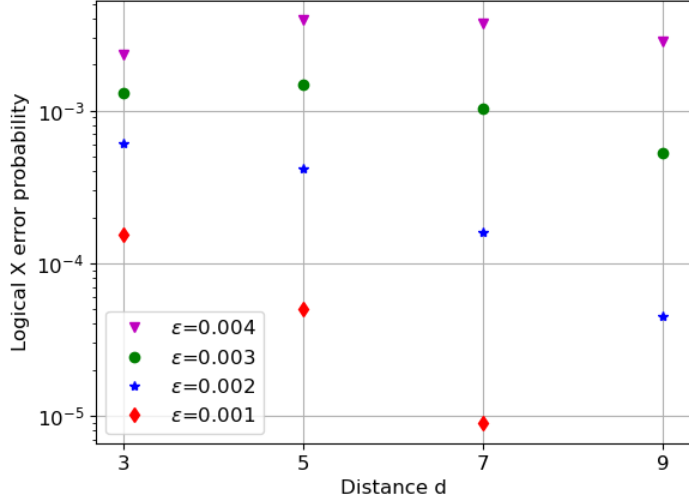


Figure 5: **Probability of a logical X error P_X** for the code switching $\mathcal{S}_1 \rightarrow \mathcal{S}_2 \rightarrow \mathcal{S}_1$ with $L = 3$ syndrome cycles for the asymmetric surface code \mathcal{S}_2 and d syndrome cycles for the regular surface code \mathcal{S}_1 . To enable efficient simulation we skipped the T -gate application in Algorithm 1. Our data suggests that logical X errors are exponentially suppressed as one increases the code distance.

that Pauli frame and logical Z errors are independent, the combined logical error rate is therefore $\bar{\varepsilon} \approx P_Z + P_F/2 \approx 30\varepsilon$ in the limit $\varepsilon \ll 1$.

4 Discussion

We conclude with a discussion how the presented combination of quantum error correction with quantum error mitigation compares to conventional quantum error correction schemes and classical simulation.

4.1 Comparison with quantum error correction and classical simulation

Using the schemes explained above we can simulate universal fault-tolerant quantum circuits with a total sampling cost $\Gamma_\varepsilon^2 = \gamma_\varepsilon^{2t}$, where t denotes the T -count of the circuit. Recalling (9) and setting the total sampling overhead Γ_ε^2 to a fixed desired value gives for $\eta := \log(\Gamma_\varepsilon^2)/(4\kappa)$

$$t = \frac{\log \Gamma_\varepsilon^2}{2 \log(1 + 2\kappa\varepsilon + O(\varepsilon^2))} = \eta/\varepsilon + O(1) \quad \text{for } \varepsilon \ll 1.$$

If we neglect the second order term in (9) we find $t \approx \eta(1/\varepsilon + \kappa)$, which is plotted in Figure 6. We see that for realistic error rates and a moderate total sampling overhead our scheme allows to simulate quantum circuits with a number of T -gates that are unfeasible for classical algorithms [4].

Table 1 compares the presented approach to conventional quantum error correction (QEC) and classical simulation. The new method comes with a simulation overhead that scales exponentially in the number of T -gates however the base of this exponential function depends on the physical error rate ε and is considerably smaller compared to the classical simulation for realistic noise levels. Hence the method may help for a smooth transition into the universal fault-tolerant quantum computing era.

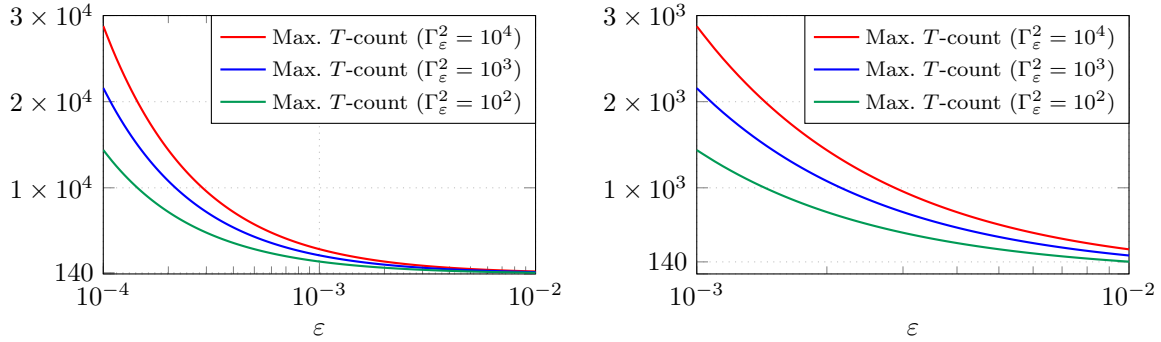


Figure 6: **Maximal T-count** that can be performed via the magic state method (see Section 2) with a total sampling cost $\Gamma_\varepsilon^2 \in \{10^2, 10^3, 10^4\}$. We assume a depolarizing noise model with only two-qubit errors, i.e., γ_ε is given in (9) for $\kappa = 2/5$, where we neglect second order error terms.

	conventional QEC	QPD assisted QEC	classical simulation
hardware requirements	FT Clifford gates & magic state factory	FT Clifford gates	classical computer
T -gate complexity	$O(t)$	γ_ε^{2t}	1.3831^t

Table 1: Comparison of the new approach with conventional quantum error correction and classical simulation.

4.2 Limitations, possible generalizations, and future work

With the usage of the QPD method in a fault-tolerant setting we inherit some of the shortcomings of this error mitigation scheme. The estimation of the logical error rate discussed in Section 2.2 needs to be sufficiently accurate and we require certain assumptions on the noise model, such as the absence of correlated errors between different realizations of error-mitigated gates and the noise not strongly changing over time. The method is also restricted to removing the bias from expected values of measurement outcomes. Furthermore, we require more accuracy on the transversal encoded gates, which is not a problem in practice. To see this, suppose for simplicity that the transversal operations are all executed without error, then the method would simulate a quantum channel $\mathcal{F}^{(\text{ideal})}$ which is a quasi-probabilistic mixture $\mathcal{F}^{(\text{ideal})} = \sum_k a_k \mathcal{E}_k^{(\text{ideal})}$ of every 'branch' $\mathcal{E}_k^{(\text{ideal})}$ of the QPD. However, even transversal operations incur an error, which can be exponentially suppressed by increasing the code distance. Therefore the actual channel that is simulated by the method will be $\mathcal{F} = \sum_k a_k \mathcal{E}_k$ where \mathcal{E}_k includes the effects from noise in the transversal gates. We can make the error $\|\mathcal{E}_k - \mathcal{E}_k^{(\text{ideal})}\| \leq \Delta$ arbitrarily small by increasing the code distance. By the triangle inequality we see that

$$\|\mathcal{F} - \mathcal{F}^{(\text{ideal})}\| \leq \sum_k |a_k| \|\mathcal{E}_k - \mathcal{E}_k^{(\text{ideal})}\| \leq \gamma_\varepsilon^{2t} \Delta,$$

where t denotes the T -count. Hence to make the overall error $\delta > 0$ on the output sufficiently small we have to choose $\Delta = \delta \gamma_\varepsilon^{-2t}$ exponentially small in the number of T -gates. Recalling that in a generic fault-tolerant setting we choose

$$n = \text{polylog}(1/\Delta, |C|) = \text{polylog}(\gamma_\varepsilon^{2t}/\delta, |C|) = \text{poly}(t, \log(1/\delta), \log(|C|)),$$

which at first sight looks disappointing, because in realistic cases where $O(|C|) = O(t)$ the code size now scales polynomially in the number of locations $|C|$, instead of polylogarithmically as in the standard fault-tolerant setting. We argue that this is not really a problem in practice, since asymptotically the QPD method is in any case less advantageous than the conventional approach using a magic state

factory. Recall that by nature of the QPD method, we only consider circuits where the total sampling overhead γ_ε^{2t} is sufficiently small, i.e., $\gamma_\varepsilon^{2t} \leq \beta$ for some constant $\beta > 0$ not too large³ we obtain $\Delta \geq \delta/\beta$ and hence

$$n = \text{polylog}(\beta/\delta, |C|). \quad (13)$$

The scaling (13) matches again what we expect from the standard fault-tolerant setting.

It is an open question for future research to figure out if and how error mitigation techniques can be efficiently used in order to mitigate non-transversal gates beyond the T -gate. The two methods proposed in this paper cannot be directly generalized to arbitrary non-transversal gates, as the procedure of twirling the noise relies on the fact that the T -gate lies in the third Clifford hierarchy. However, if one were to forgo the tayloring of the noise to a Pauli channel, the code switching method could be used to implement an arbitrary noisy R_z rotation. This comes with the drawback that the characterization of the (possibly coherent) noise would presumably require a full tomography procedure, which is significantly less efficient than the exponential fitting method described in Section 2.2.⁴

In the near future one might encounter the situation where we lack the resources to distill magic states to sufficiently high fidelity that allows for large-scale fault-tolerant computation with T -gates, but a few rounds of distillation might still provide states that are better than raw noisy magic states. In that case one could combine distillation with error mitigation allowing for a trade-off between resources spent on distillation and the sampling overhead, by tuning how many distillation steps are performed.

Note During the preparation of this work, we became aware of an independent effort to use error mitigation for universal quantum computing via encoded Clifford+ T circuits [10].

Acknowledgements We thank Stefan Woerner for helpful comments and discussions. Part of this work was done when CP was a research intern at IBM Research Zurich. CP acknowledges support from the Swiss National Science Foundation via the National Centre of Competence in Research QSIT. SB is supported in part by the IBM Research Frontiers Institute.

References

- [1] S. Aaronson and D. Gottesman. Improved simulation of stabilizer circuits. *Phys. Rev. A*, 70:052328, 2004. [DOI: 10.1103/PhysRevA.70.052328](https://doi.org/10.1103/PhysRevA.70.052328).
- [2] D. Aharonov and M. Ben-Or. Fault-tolerant quantum computation with constant error rate. *SIAM J. Comput.*, 38(4):1207–1282, 2008. [DOI: 10.1137/S0097539799359385](https://doi.org/10.1137/S0097539799359385).
- [3] M. E. Beverland, O. Buerschaper, R. Koenig, F. Pastawski, J. Preskill, and S. Sijher. Protected gates for topological quantum field theories. *Journal of Mathematical Physics*, 57(2):022201, 2016. [DOI: 10.1063/1.4939783](https://doi.org/10.1063/1.4939783).
- [4] S. Bravyi and D. Gosset. Improved classical simulation of quantum circuits dominated by Clifford gates. *Phys. Rev. Lett.*, 116:250501, 2016. [DOI: 10.1103/PhysRevLett.116.250501](https://doi.org/10.1103/PhysRevLett.116.250501).
- [5] S. Bravyi, D. Gosset, R. Koenig, and M. Tomamichel. Quantum advantage with noisy shallow circuits. *Nature Physics*, 16(10):1040–1045, 2020. [DOI: 10.1038/s41567-020-0948-z](https://doi.org/10.1038/s41567-020-0948-z).
- [6] S. Bravyi and A. Kitaev. Universal quantum computation with ideal Clifford gates and noisy ancillas. *Phys. Rev. A*, 71:022316, 2005. [DOI: 10.1103/PhysRevA.71.022316](https://doi.org/10.1103/PhysRevA.71.022316).

³If β would be too large then the sampling overhead would make the QPD method infeasible.

⁴It has been shown that an arbitrary noise channel can always be expressed in terms of a quasi-probabilistic mixture of operations consisting of Clifford gates and measurements in the computational basis [14].

- [7] S. Bravyi and A. Vargo. Simulation of rare events in quantum error correction. *Phys. Rev. A*, 88:062308, 2013. [DOI: 10.1103/PhysRevA.88.062308](https://doi.org/10.1103/PhysRevA.88.062308).
- [8] C. D. Bruzewicz, J. Chiaverini, R. McConnell, and J. M. Sage. Trapped-ion quantum computing: Progress and challenges. *Applied Physics Reviews*, 6(2):021314, 2019. [DOI: 10.1063/1.5088164](https://doi.org/10.1063/1.5088164).
- [9] A. R. Calderbank and P. W. Shor. Good quantum error-correcting codes exist. *Phys. Rev. A*, 54:1098–1105, 1996. [DOI: 10.1103/PhysRevA.54.1098](https://doi.org/10.1103/PhysRevA.54.1098).
- [10] A. Ciani and M. Lostaglio. personal communication.
- [11] A. D. Córcoles, A. Kandala, A. Javadi-Abhari, D. T. McClure, A. W. Cross, K. Temme, P. D. Nation, M. Steffen, and J. M. Gambetta. Challenges and opportunities of near-term quantum computing systems. *Proceedings of the IEEE*, 108(8):1338–1352, 2020. [DOI: 10.1109/JPROC.2019.2954005](https://doi.org/10.1109/JPROC.2019.2954005).
- [12] E. Dennis, A. Kitaev, A. Landahl, and J. Preskill. Topological quantum memory. *Journal of Mathematical Physics*, 43(9):4452–4505, 2002. [DOI: 10.1063/1.1499754](https://doi.org/10.1063/1.1499754).
- [13] B. Eastin and E. Knill. Restrictions on transversal encoded quantum gate sets. *Phys. Rev. Lett.*, 102:110502, 2009. [DOI: 10.1103/PhysRevLett.102.110502](https://doi.org/10.1103/PhysRevLett.102.110502).
- [14] S. Endo, S. C. Benjamin, and Y. Li. Practical quantum error mitigation for near-future applications. *Phys. Rev. X*, 8:031027, 2018. [DOI: 10.1103/PhysRevX.8.031027](https://doi.org/10.1103/PhysRevX.8.031027).
- [15] A. G. Fowler, A. M. Stephens, and P. Groszkowski. High-threshold universal quantum computation on the surface code. *Phys. Rev. A*, 80:052312, 2009. [DOI: 10.1103/PhysRevA.80.052312](https://doi.org/10.1103/PhysRevA.80.052312).
- [16] V. Havlíček, A. D. Córcoles, K. Temme, A. W. Harrow, A. Kandala, J. M. Chow, and J. M. Gambetta. Supervised learning with quantum-enhanced feature spaces. *Nature*, 567(7747):209–212, 2019. [DOI: 10.1038/s41586-019-0980-2](https://doi.org/10.1038/s41586-019-0980-2).
- [17] C. Horsman, A. G. Fowler, S. Devitt, and R. V. Meter. Surface code quantum computing by lattice surgery. *New Journal of Physics*, 14(12):123011, 2012. [DOI: 10.1088/1367-2630/14/12/123011](https://doi.org/10.1088/1367-2630/14/12/123011).
- [18] P. Jurcevic et al. Demonstration of quantum volume 64 on a superconducting quantum computing system. *Quantum Science and Technology*, 2021. [DOI: 10.1088/2058-9565/abe519](https://doi.org/10.1088/2058-9565/abe519).
- [19] A. Kandala, A. Mezzacapo, K. Temme, M. Takita, M. Brink, J. M. Chow, and J. M. Gambetta. Hardware-efficient variational quantum eigensolver for small molecules and quantum magnets. *Nature*, 549(7671):242–246, 2017. [DOI: 10.1038/nature23879](https://doi.org/10.1038/nature23879).
- [20] A. Kandala, K. Temme, A. D. Córcoles, A. Mezzacapo, J. M. Chow, and J. M. Gambetta. Error mitigation extends the computational reach of a noisy quantum processor. *Nature*, 567(7749):491–495, 2019. [DOI: 10.1038/s41586-019-1040-7](https://doi.org/10.1038/s41586-019-1040-7).
- [21] S. Khatri, R. LaRose, A. Poremba, L. Cincio, A. T. Sornborger, and P. J. Coles. Quantum-assisted quantum compiling. *Quantum*, 3:140, 2019. [DOI: 10.22331/q-2019-05-13-140](https://doi.org/10.22331/q-2019-05-13-140).
- [22] A. Kitaev. Anyons in an exactly solved model and beyond. *Annals of Physics*, 321(1):2 – 111, 2006. [DOI: https://doi.org/10.1016/j.aop.2005.10.005](https://doi.org/10.1016/j.aop.2005.10.005). January Special Issue.
- [23] Y. Li. A magic state’s fidelity can be superior to the operations that created it. *New Journal of Physics*, 17(2):023037, 2015. [DOI: 10.1088/1367-2630/17/2/023037](https://doi.org/10.1088/1367-2630/17/2/023037).
- [24] Y. Li and S. C. Benjamin. Efficient variational quantum simulator incorporating active error minimization. *Phys. Rev. X*, 7:021050, 2017. [DOI: 10.1103/PhysRevX.7.021050](https://doi.org/10.1103/PhysRevX.7.021050).

[25] J. Lodyga, P. Mazurek, A. Grudka, and M. Horodecki. Simple scheme for encoding and decoding a qubit in unknown state for various topological codes. *Scientific Reports*, 5(1):8975, 2015. [DOI: 10.1038/srep08975](https://doi.org/10.1038/srep08975).

[26] S. McArdle, T. Jones, S. Endo, Y. Li, S. C. Benjamin, and X. Yuan. Variational ansatz-based quantum simulation of imaginary time evolution. *npj Quantum Information*, 5(1):75, 2019. [DOI: 10.1038/s41534-019-0187-2](https://doi.org/10.1038/s41534-019-0187-2).

[27] K. Mitarai, Y. O. Nakagawa, and W. Mizukami. Theory of analytical energy derivatives for the variational quantum eigensolver. *Phys. Rev. Research*, 2:013129, 2020. [DOI: 10.1103/PhysRevResearch.2.013129](https://doi.org/10.1103/PhysRevResearch.2.013129).

[28] J. E. Moussa. Transversal Clifford gates on folded surface codes. *Phys. Rev. A*, 94:042316, 2016. [DOI: 10.1103/PhysRevA.94.042316](https://doi.org/10.1103/PhysRevA.94.042316).

[29] P. J. J. O’Malley et al. Scalable quantum simulation of molecular energies. *Phys. Rev. X*, 6:031007, 2016. [DOI: 10.1103/PhysRevX.6.031007](https://doi.org/10.1103/PhysRevX.6.031007).

[30] A. Paetznick and B. W. Reichardt. Universal fault-tolerant quantum computation with only transversal gates and error correction. *Phys. Rev. Lett.*, 111:090505, 2013. [DOI: 10.1103/PhysRevLett.111.090505](https://doi.org/10.1103/PhysRevLett.111.090505).

[31] H. Pashayan, O. Reardon-Smith, K. Korzekwa, and S. D. Bartlett. Fast estimation of outcome probabilities for quantum circuits, 2021. Available online: <https://arxiv.org/abs/2101.12223>.

[32] A. Peruzzo, J. McClean, P. Shadbolt, M.-H. Yung, X.-Q. Zhou, P. J. Love, A. Aspuru-Guzik, and J. L. O’Brien. A variational eigenvalue solver on a photonic quantum processor. *Nature Communications*, 5(1), 2014. [DOI: 10.1038/ncomms5213](https://doi.org/10.1038/ncomms5213).

[33] E. Peters, J. Caldeira, A. Ho, S. Leichenauer, M. Mohseni, H. Neven, P. Spentzouris, D. Strain, and G. N. Perdue. Machine learning of high dimensional data on a noisy quantum processor, 2021. Available online: <https://arxiv.org/abs/2101.09581>.

[34] C. Piveteau, D. Sutter, and S. Woerner. Quasiprobability decompositions with reduced sampling overhead, 2021. Available online: <https://arxiv.org/abs/2101.09290>.

[35] M. Schuld and N. Killoran. Quantum machine learning in feature Hilbert spaces. *Phys. Rev. Lett.*, 122:040504, 2019. [DOI: 10.1103/PhysRevLett.122.040504](https://doi.org/10.1103/PhysRevLett.122.040504).

[36] P. W. Shor. Scheme for reducing decoherence in quantum computer memory. *Phys. Rev. A*, 52:R2493–R2496, 1995. [DOI: 10.1103/PhysRevA.52.R2493](https://doi.org/10.1103/PhysRevA.52.R2493).

[37] P. W. Shor. Fault-tolerant quantum computation. In *Proceedings of 37th Conference on Foundations of Computer Science*, pages 56–65, 1996. [DOI: 10.1109/SFCS.1996.548464](https://doi.org/10.1109/SFCS.1996.548464).

[38] A. Steane. Multiple-particle interference and quantum error correction. *Proceedings of the Royal Society of London. Series A: Mathematical, Physical and Engineering Sciences*, 452(1954):2551–2577, 1996. [DOI: 10.1098/rspa.1996.0136](https://doi.org/10.1098/rspa.1996.0136).

[39] A. M. Steane. Error correcting codes in quantum theory. *Phys. Rev. Lett.*, 77:793–797, 1996. [DOI: 10.1103/PhysRevLett.77.793](https://doi.org/10.1103/PhysRevLett.77.793).

[40] K. Temme, S. Bravyi, and J. M. Gambetta. Error mitigation for short-depth quantum circuits. *Phys. Rev. Lett.*, 119(18), 2017. [DOI: 10.1103/physrevlett.119.180509](https://doi.org/10.1103/physrevlett.119.180509).